Exploring different carbon allotrope thermoplastic composites for electrochemical sensing

*Khalil K. Hussain[1,2], Ricoveer Singh Shergill[1,2], Hairul Hisham Hamzah[3], Mark S. Yeoman[1,2], Bhavik A. Patel[1,2]**

[1]School of Applied Sciences, University of Brighton, Brighton, BN2 4GJ, UK

[2]Centre for Stress and Age-Related Diseases, University of Brighton, Brighton, BN2 4GJ, UK

[3]School of Chemical Sciences, Universiti Sains Malaysia, 11800, Gelugor Penang, Malaysia

KEYWORDS: Carbon thermoplastic, carbon allotropes, 3D printing, electrochemical sensors, serotonin.

ABSTRACT

Composite electrodes are an effective and cheap way to utilise a wide range of carbon materials to make electrodes. More recently thermoplastics have been widely used as the binder to make carbon composite electrodes, as varying fabrication approaches, such as 3D printing, can make highly reproducible electrodes. However, there is a clear need to understand how the electrochemical performance of different carbon allotrope materials varies when made into sensors. We accessed polylactic acid (PLA) thermoplastic filaments containing carbon black, graphite, graphene, multiwall carbon nanotube (MWCNT) and carbon fiber using various electrochemical techniques. Graphite/PLA and graphene/PLA electrodes showed the best electron transfer kinetics. Graphene/PLA electrodes had the greatest sensitivity and lowest limit of detection for the measurement of serotonin. CB/PLA was least prone to electrode fouling from oxidative by-product generated from the oxidation of serotonin. 3D printing was used to make various carbon allotrope materials into complex shapes to evaluate the batch uniformity of the printed parts. Of all the materials explored, CB/PLA had the best resolution and batch uniformity when compared to PLA. Overall, our study highlights that the type of the carbon allotrope plays as much influence as amount of carbon on the electrochemical performance of carbon thermoplastic electrodes. These findings will provide significant guidance on the appropriate choice of carbon thermoplastic composite materials when designing electrodes for a wide range of applications.

INTRODUCTION

Carbon electrodes have been used in a wide and diverse range of applications such as fuel cells, environmental treatments, biosensors, and chemical sensors[1-7]. This is mainly because carbon electrodes have been shown to have high conductivity, good chemical stability, biocompatibility, and low cost[8-9]. However, the major challenge with carbon-based electrodes is the balance between electrochemical activity and the simplicity of making electrodes. These challenges on fabrication have become more problematic as applications require the development of more complex electrode geometries. Therefore, there remains a significant interest in carbon electrodes that are easy to fabricate, have high electrochemical activity and can be made in varying sizes and shapes with high precision.

Since their conception, composite electrodes have provided a simple and effective way to utilise a wide breadth of carbon material to make millimeter sized electrode structures[10-13]. Composite electrodes are made from carbon particles held together using a form of binder. Traditionally binders consisted of wax[14], epoxy resins[15-17] or plastics such as Teflon[13, 18]. Whilst these are easy to make, it is difficult to make smaller and complex geometry electrodes. Therefore, recently thermoplastics such as poly (methyl-methacrylate)[19-20] and poly lactic acid (PLA)[21-22] have been more widely used as binders and studies have shown these can be patterned and molded to make sub-millimeter sized electrodes[20, 23-25]. Further developments have been achieved through the utilization of carbon composite thermoplastics in 3D printing, which has provided the scope to fabricate electrodes of complex geometries[26-30]. Although a host of studies have explored the potential of carbon thermoplastic composite conductive electrodes[26, 31-33], it is generally unclear how the performance of different carbon thermoplastic materials varies when assessed for electrochemical sensing.

Within this study, we present a comprehensive exploration of different carbon allotrope thermoplastic materials for generating electrodes. We compared carbon black/PLA, graphite/PLA, graphene/PLA, multiwall carbon nanotube (MWCNT)/PLA and carbon fiber/PLA molded electrodes. We evaluated the electrodes using inner- and outer- sphere redox probes using cyclic voltammetry. Following this we evaluated the sensing potential of the materials by conducting measurements to explore the sensitivity and stability to measure serotonin. Lastly, we explored how two different printed parts were made using the different carbon allotropes compared to PLA in terms of printing resolution and batch reproducibility. Overall, our study highlights the scope of these materials for electrochemical sensing.

RESULTS & DISCUSSION

The percentage weight of carbon within the commercial carbon composite thermoplastic varied (Table 1), with carbon black/PLA filament containing the highest percentage of carbon and the carbon fiber/PLA filament containing the lowest.

Table 1. The percentage weight of carbon present within the conductive thermoplastic materials and the resistance measured of the electrode utilised for electrochemical measurements.

Material	Carbon weight (%)	Resistivity (kΩ m)
Carbon black / PLA	45.4 ± 8.6	4.0 ± 0.3
Graphite / PLA	25.4 ± 3.1	0.9 ± 0.2
Graphene / PLA	21.3 ± 4.2	2.6 ± 0.4
MWCNT / PLA	14.0 ± 5.5	33.7 ± 3.7
Carbon fiber / PLA	9.3 ± 3.2	Not measurable

The resistivity of the cylinder electrode which was filled using a 3D pen was measured. This approach was taken as molding is one of the most effective ways to make electrodes using carbon thermoplastics[34-38]. The electrode depth was 1.2 mm and the diameter was 2 mm. From Table 1, there was no significant difference in resistivity of CB/PLA, graphite/PLA and graphene/PLA (one way ANOVA). This suggests that even with variations in percentage of carbon, the distribution of the carbon material within the thermoplastic may play a key role in determining the conductivity of the material. There was a significant increase in resistivity of MWCNT/PLA when compared to all materials ($p<0.001$), which is most likely due to such a low percentage of carbon present in the thermoplastic. No resistivity could be measured in carbon fiber/PLA.

To further evaluate the different materials, SEM images were taken of the residues of the carbon allotrope thermoplastic filaments to explore the carbon structures present within the filament and particle size distribution was using a Mastersizer. Supplementary Figure 1 shows SEM of the residues of the different filaments, where larger clumps of material were observed in CB and

graphite, with sheet-like structures evident in the latter. The presence of graphene sheets of varying sizes was observed, of which these were often stacked into agglomerated particles. Within the MWCNT/PLA filament, there were clusters of nanotubes present with diameters in the range of 20 -50 nm. We did not observe other carbon-based impurities in the materials from SEM studies. Figure 1 shows particle size distribution, where the median particle size by volume was 217 ± 21 μm for CB, 163 ± 40 μm for graphite, 152 ± 42 μm for graphene and 59 ± 26 μm for MWCNT (n = 3). There was a significant increase in the median particle size by volume in CB when compared to graphene ($p<0.05$) and MWCNT ($p<0.001$, n=3). Median particle size by volume was significant smaller in MWCNT when compared to graphite ($p<0.05$, Figure 1). These variations in the particle sizes can influence the probability of forming conductive pathways which in turn can impact the conductivity of the carbon thermoplastic filament. Additional different carbon materials have been shown to have varying electronic properties[8], with studies highlighting graphene and carbon nanotubes can show enhanced electrocatalytic behaviour[39-41] and determination of analytes that adsorb onto the electrode surface for electron transfer[42-43].

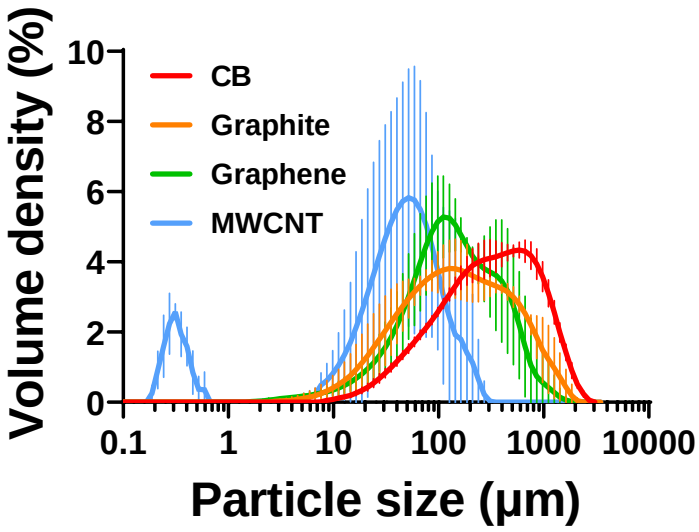

Figure 1. Particle size distribution of different carbon allotrope thermoplastic filaments. Data shown as mean ± S.D., n=3

Supplementary Figure 2 shows Energy-dispersive X-ray spectroscopy (EDS) analysis showing the presence of trace metals Fe and Mg in graphite/PLA and Fe and Al in MWCNT/PLA. No trace metals were observed in CB/PLA and graphene/PLA filaments. The impact of trace metals has been previously known to enhance the electrochemical activity of carbon thermoplastic materials[44-45].

Cyclic voltammetry responses of the outer sphere redox probe ruthenium hexamine are shown in Figure 2A. To compare between the current responses, the cathodic peak current was normalised by the percentage weight of carbon present in each different carbon allotrope electrode. No detectable current was observed on the carbon fiber/PLA (Figure 2A). There was a significant increase in the normalised cathodic peak current response on graphene/PLA electrodes when compared to CB/PLA, graphite/PLA and MWCNT/PLA electrodes ($p<0.001$, n=8, Figure 2B).

However, the variance in the current responses was greatest on the graphene/PLA electrodes. The normalised cathodic peak current was significantly greater on MWCNT/PLA and graphite/PLA electrodes when compared to and CB/PLA electrodes ($p<0.001$, $n=8$, Figure 2B). The difference between the anodic and cathodic peak potential (ΔE), which provides insight into the electron transfer kinetics for the different carbon allotrope materials. The ΔE was significantly increased on MWCNT/PLA electrodes when compared to CB/PLA, graphite/PLA and graphene/PLA electrodes (all $p<0.001$, $n=8$, Figure 2C). The ΔE significantly increased for graphene/PLA electrodes when compared to CB/PLA electrodes and graphite/PLA electrodes (all $p<0.001$, $n=8$, Figure 2C). These findings indicate that faster electron transfer is most likely to be observed on CB/PLA and graphite/PLA for outer sphere redox probes.

Cyclic voltammetry responses were obtained using the inner sphere redox probe ferricyanide on the different electrodes (Figure 2D), where once again no response was observed for carbon fiber/PLA electrodes. The normalised anodic peak current was significantly greater in graphene/PLA electrodes when compared to CB/PLA ($p<0.001$), graphite/PLA ($p<0.01$) and MWCNT/PLA electrodes ($p<0.001$, $n=8$, Figure 2E). The normalised anodic peak current was significantly greater on MWCNT/PLA and graphite/PLA electrodes when compared to and CB/PLA electrodes ($p<0.001$, $n=8$, Figure 2E). These changes were like those observed with ruthenium hexamine. The ΔE was significantly greater on MWCNT/PLA electrodes when compared to CB/PLA, graphite/PLA and graphene/PLA electrodes (all $p<0.001$, $n=8$, Figure 2F). The ΔE was significantly greater on CB/PLA electrodes when compared to graphite/PLA and graphene/PLA electrodes (both $p<0.01$, $n=8$, Figure 2F).

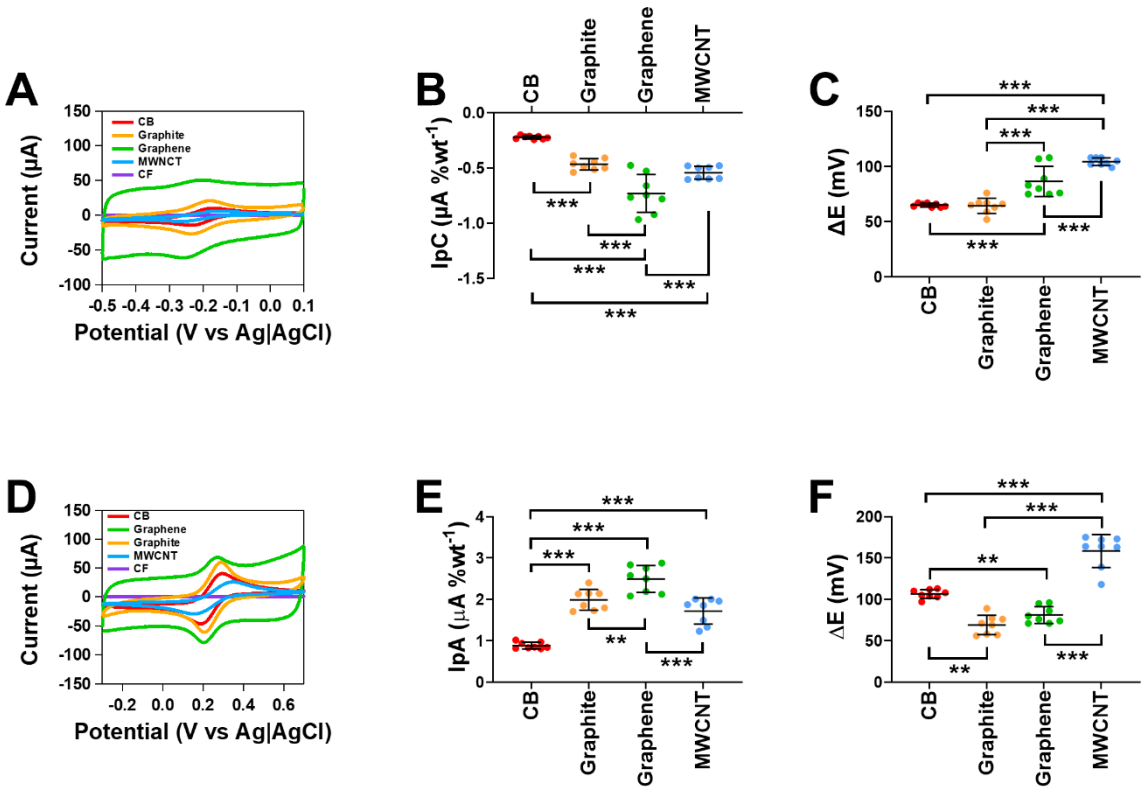

Figure 2. Investigation of different carbon allotrope thermoplastic electrodes on outer and inner sphere redox probes. (A) Cyclic voltammograms of 1 mM ruthenium hexamine in 1 M KCl on the different carbon allotrope thermoplastics. (B) Normalised cathodic peak current and (C) difference between the anodic and cathodic peak potentials (ΔE) for ruthenium hexamine. (D) Cyclic voltammograms of 1 mM ferricyanide in 1 M KCl on the different carbon allotrope thermoplastics. (E) Normalised anodic peak current and (F) difference between the anodic and cathodic peak potentials (ΔE) for ferricyanide. Data shown as mean ± S.D., n=8, **p<0.01 and ***p<0.001

To study the electron transfer resistance of the different carbon allotrope thermoplastic electrodes, electrochemical impedance spectroscopy (EIS) measurements were conducted. Figure 3A shows the Nyquist plots for all the different electrodes. Responses for graphite/PLA and

graphene/PLA electrodes were dominated by Warburg lines, suggestive of a process that is governed by mass transport. The semicircle for MWCNT/PLA was greater than that observed for CB/PLA, which indicates poor electron transfer kinetics. These findings strongly support the observations on the redox probes in Figure 2. To obtain the Rct values from the Nyquist plots, the experimental data was fitted using electrical circuits as shown in Supplementary Figure 3. Figure 3B shows Bode plots, which confirm the suitability of these electrical circuits for fitting our EIS data. The resultant Rct values from the fitted electrical circuits were obtained and are shown for the different carbon allotrope thermoplastic electrodes in Figure 3C. There was a significant increase in Rct on MWCNT/PLA electrodes when compared to all other materials ($p<0.001$, $n=8$). The Rct was slightly higher in CB/PLA electrodes when compared to graphite/PLA and graphene/PLA electrodes. Our findings are like those observed from studies conducted using commercial carbon allotrope thermoplastics[46-50], but recent studies have shown Rct can be reduced through the fabrication of in-house filaments with varying loads of carbon [51-52].

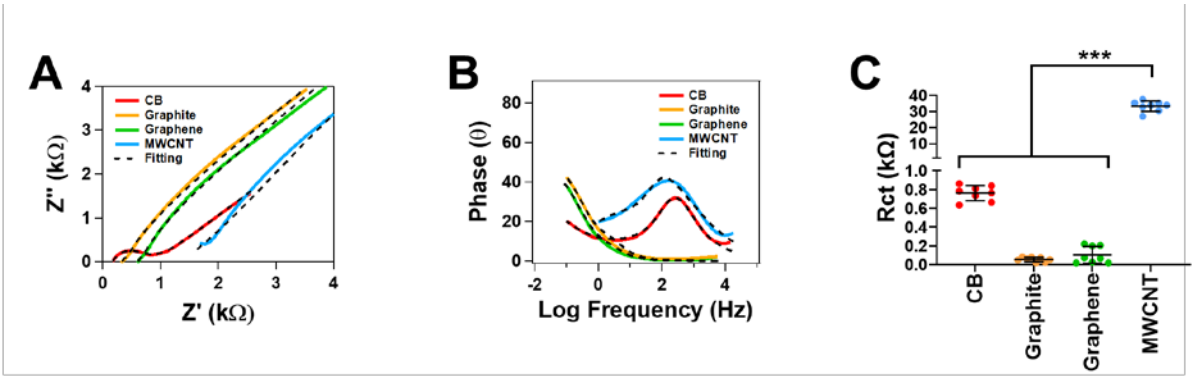

Figure 3. Electrochemical impedance spectra of conductive carbon allotrope thermoplastic electrodes. (A) Nyquist plot and (B) Bode plot. All experimental data was fitted using electrical circuits, in which (C) Rct values were obtained. The measurements were carried out in 5 mM ferricyanide and 5 mM ferrocyanide

mixture solution 1 M KCl at a modulation amplitude of 5 mV and a frequency range of 20000 Hz to 0.01 Hz. Data shown as mean ± SD; $n = 8$; ***$p < 0.001$.

Our findings from the redox probe and EIS measurements highlight that the percentage of carbon present within the electrode does not completely dictate the performance, but the type of carbon allotrope also has a significant influence. Although the widest used material[53-55], CB/PLA (which contains the greatest amount of carbon) had the lowest normalised current response when compared to all other carbon allotropes. CB/PLA electrodes also would have a lower current to graphite/PLA and graphene/PLA without normalizing the current responses for the amount of carbon present. There is a clear threshold in the amount of the carbon present and its influence on electron transfer kinetics, with MWCNT/PLA electrodes having the highest ΔE and Rct, and thus poor electron transfer kinetics. Once again CB/PLA electrodes had a higher ΔE and Rct than graphite/PLA and graphene/PLA on the inner sphere redox probe again potentially highlight that the type of carbon allotrope plays a critical contribution to the electrochemical activity of the electrode. These findings highlight that above a particular threshold of carbon amount (> 20 %) within the thermoplastic the type of carbon allotrope dominate the electrochemical behavior of the material.

Given the interesting findings from the redox probe, we explored the sensing capabilities of the different carbon allotrope thermoplastic electrodes were explored. Electrodes were evaluated for the determination of 5-HT, which is an important neurotransmitter that plays key roles in signalling within the central and peripheral nervous system and thus is of key interest for stable monitoring[56-

[60]. Our previous studies have shown that micromolar concentration of these molecules have been detected from biological tissues[35, 61-62].

Differential pulse voltammograms of 5-HT at concentrations from 2 to 10 µM were obtained on CB/PLA (Figure 4A), graphite/PLA (Figure 4B) graphene/PLA (Figure 4C) and MWCNT/PLA (Figure 4D) electrodes. The normalized calibration responses for all materials are shown in Figure 4E, where clear linear responses were observed over the concentration range of 5-HT. Table 2 shows the sensitivity, limit of detection (LOD) and limit of quantification (LOQ) for the measurement of 5-HT on the different carbon allotrope thermoplastic electrodes.

Table 2. Sensitivity and detection limits for the detection of 5-HT on the various carbon allotrope thermoplastic electrodes, where n=6. For sensitivity values, the current was initially normalised by the % weight of carbon present within each filament.

Material	**Sensitivity (nA %wt μM^{-1})**	**Limit of detection (LOD, µM)**	**Limit of qualification (LOQ, µM)**
Carbon black / PLA	2.1	1.1	3.4
Graphite / PLA	7.7	1.3	3.9
Graphene / PLA	14.3	0.2	0.7
MWCNT / PLA	2.7	0.8	2.3

Overall, the greatest sensitivity and lowest LOD for the measurement of 5-HT was observed on graphene/PLA electrodes. MWCNT/PLA electrodes had the second best LOD which is surprising given the low percentage of carbon present. These findings further support the unique properties

of graphene and MWCNT outweigh having higher percentage load of carbon as observed in CB/PLA electrodes. Previous studies have also shown that graphene and MWCNT provide sensitive detection of 5-HT when compared to other carbon allotropes[40, 63-65].

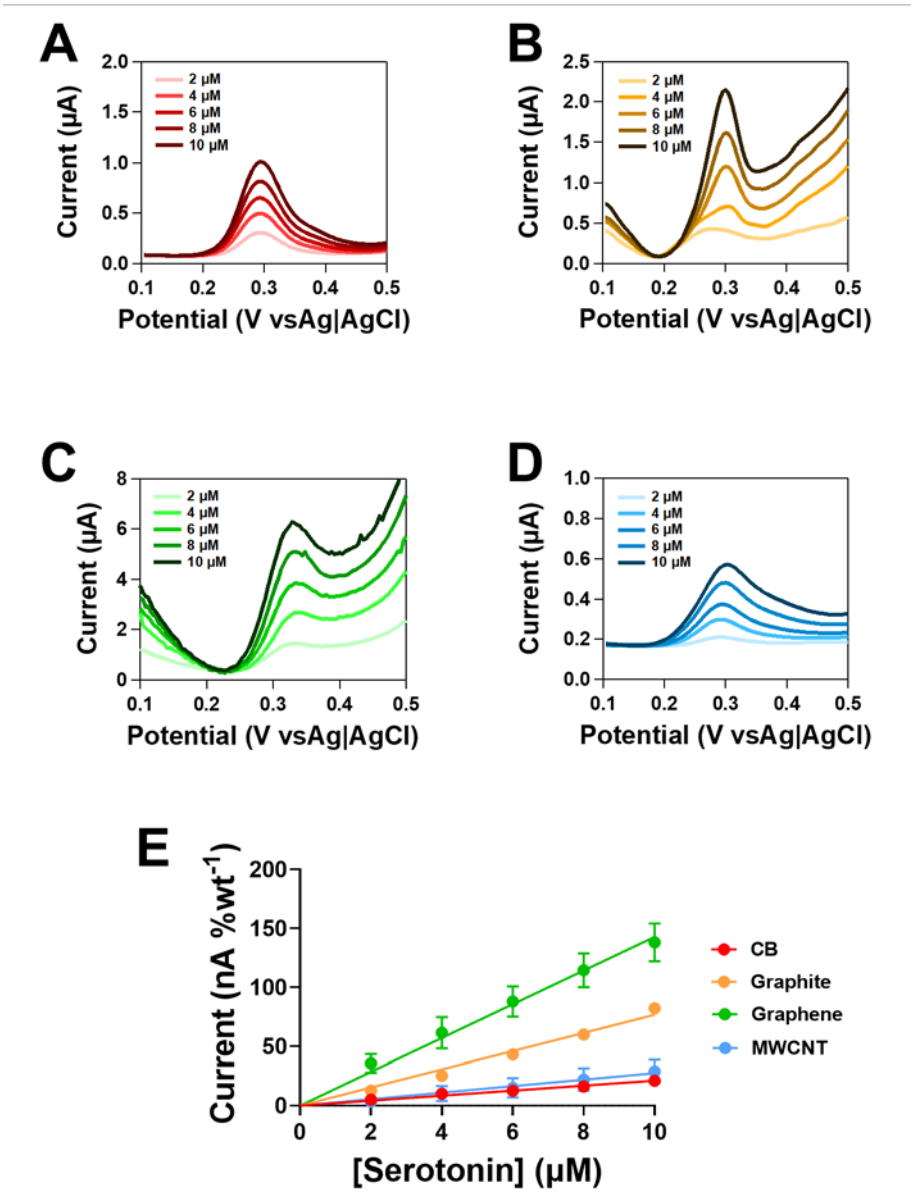

Figure 4. Relationship between concentration of serotonin (5-HT) and current response on different carbon allotrope thermoplastic electrodes. Differential pulse voltammograms of 2 – 10 µM 5-HT from (A) CB/PLE, (B) graphite/PLA, (C) graphene/PLA and (D) MWCNT/PLA electrodes. (E) shows normalised

current versus concentration calibration response of 5-HT for the different carbon allotrope thermoplastic electrodes. Data shown as mean ± S.D and n=6

Fouling studies were conducted to explore the stability of the various carbon allotrope thermoplastic electrodes for continuous monitoring of 5-HT. Oxidation of 5-HT has been shown to generate by-products which have an affinity to stick onto the carbon material on the electrode surface and diminish the current response over time[66-68]. For measurements, the reduction peak current of redox probe ruthenium hexamine was measured as a marker of the degree of electrode fouling following exposure to 5 µM 5-HT every 50 s (Figure 5). Differential pulse voltammograms of ruthenium hexamine following exposure to 5-HT at varying time points are shown on CB/PLA (Figure 5A), graphite/PLA (Figure 5B) graphene/PLA (Figure 5C) and MWCNT/PLA electrodes (Figure 5D). The overall percent loss in the ruthenium hexamine current response following exposure to 5-HT is shown in Figure 5E. For CB/PLA electrodes there was a significant reduction in the current at 250 s when compared to the initial response ($p<0.05$, n=6). For graphite/PLA electrodes, there was a significant decrease in the current when compared to the initial response at 50 s, 100 s (both $p<0.01$), 150 s, 200 s and 250 s ($p<0.001$, n=6). For graphene/PLA electrodes there was a significant decrease in the current when compared to the initial response at 100 s ($p<0.05$), 150 s ($p<0.01$), 200 s and 250 s ($p<0.001$, n=6). Lastly, for MWCNT/ PLA electrodes there was a significant decrease in the current when compared to the initial response at 50 s, 100 s (both $p<0.05$), 150 s, 200 s (both $p<0.01$) and 250 s ($p<0.001$, n=6). Overall, from our studies, CB/PLA electrodes were shown to be the most stable for sustained monitoring of 5-HT, as no significant differences in the current were observed for up to 200 s. This material has been shown to be stable previously for measurement in complex biological environments[55, 69]. For all other

materials, there was a loss in the current response within 50 to 100 s, indicating poor stability. This was slightly surprising for MWCNT and graphene, given both materials have been indicated to provide improved stability for sustained monitoring of neurotransmitters, but this reduced performance may be due to the behaviour of these carbon allotropes as composites. The graphite/PLA electrode was subject to the greatest degree of electrode fouling, which was expected as graphitic materials have been shown to be prone to fouling from oxidative by-products of 5-HT[70].

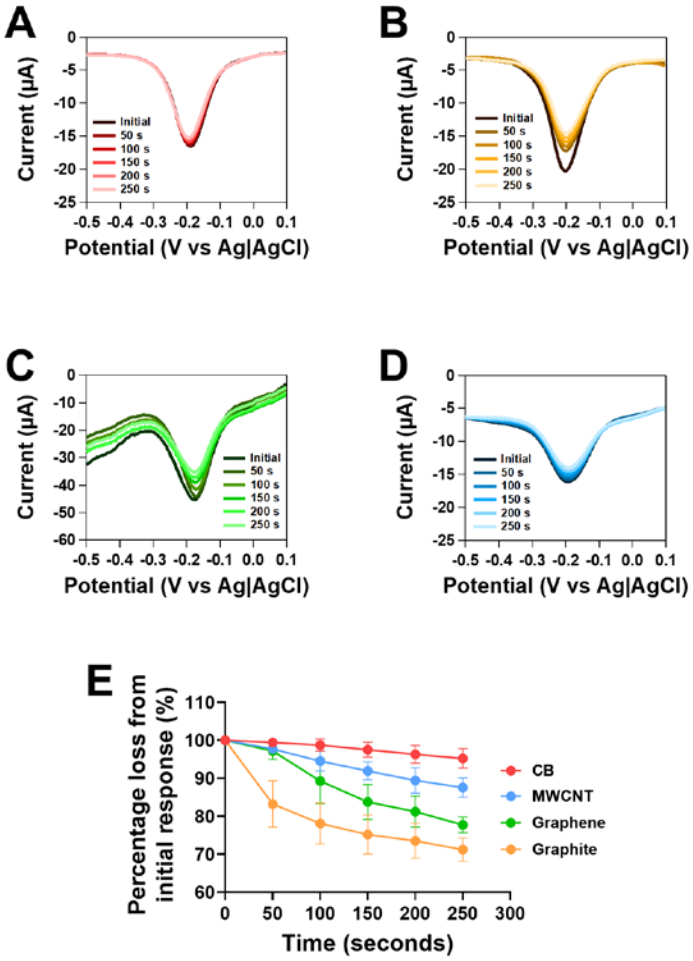

Figure 5. Stability of carbon allotrope thermoplastic electrodes for detection of 5 µM serotonin (5-HT). Differential pulse voltammograms of 1 mM ruthenium hexamine were obtained after varying durations that the electrodes were exposed to 5 µM 5-HT using amperometry at +0.65 V vs Ag|AgCl. Responses are shown on (A) CB/PLA, (B) graphite/PLA, (C) graphene/PLA and (D) MWNCT/PLA electrodes. Overall fouling data for the different electrodes is shown in (E) Data shown as mean ± S.D and n=6.

Many published studies have made carbon thermoplastic shapes as cylinders or rectangles[19-20, 71]. More recently, carbon thermoplastics have been made into sensors using 3D printing[22, 26, 30], which offers more scope in the geometries which can be made at high precision. Therefore, the printability of the different carbon allotrope thermoplastic to make different shapes was investigated (Figure 6). Materials were printed into two different designs. Firstly, we made a complex star design to investigate which material could provide the best-defined printed part when compared to PLA. We then made multiple domes, which were used to understand the reproducibility of printing the same shape. Of all the materials utilised, graphite/PLA and graphene/PLA were the hardest materials to print due to the brittle nature of the filament and had the roughest print lines. Figure 6A shows optical microscopy images of the front and back of a printed star shape on PLA and all the different carbon allotrope thermoplastics. The best definition of the shape when compared to the PLA print was achieved on CB/PLA. There was a clear definition of the star shape on all materials. The raised shapes within the star were also present in all materials but well defined in CB/PLA and graphene/PLA. In all cases cob-line features known as stringing[72] was present in all materials, mainly observed between some of the small internal shapes within the star. This occurs when the printer extruder leaks some of the filament in a region where material should not be present. In all the carbon allotrope thermoplastic materials, there

were gaps present around the edges of the star. When looking at the back of the printed part, the print lines can be observed in which CB/PLA and MWCNT/PLA were closest to that of PLA.

Figure 6B shows optical microscopy images of a printed dome, made using print layers of 100 µm to provide the best resolution of the shape[73]. The best definition of the printing layers to form the dome structure was observed on the CB/PLA and graphite/PLA when compared to PLA. To explore the uniformity of the different carbon allotrope thermoplastic materials to repeatedly print the same shape, a batch of 16 domes were printed. Image analysis was conducted to measure the surface area from the side on 2D image of each dome. Figure 6C shows that the surface area of graphene/PLA domes were significantly higher than PLA ($p<0.01$), CB/PLA ($p<0.05$) and MWCNT/PLA domes ($p<0.01$, $n=16$). The surface area of graphite/PLA domes were significantly higher than MWCNT/PLA domes ($p<0.01$, $n=16$). Although there are no differences in the absolute height and width of the domes, the differences observed in area are due to variations in the printing definition of each layer as the shape of the dome is defined and stringing effects. In terms of batch precision (Figure 6C), the percentage relative standard deviation (% RSD) was lowest for CB/PLA PEs (7.2 %, $n=16$), followed by MWCNT/PLA PEs (11.5 %), graphite/PLA PEs (11.9 %) and graphene/PLA PEs (11.9 %, $n=16$). In comparison, PLA printed domes had a %RSD of 3.8 % and thus suggestive that addition of carbon into the thermoplastic increases the print variability. This may be due to the homogeneity of the carbon particles within the thermoplastic filament. Overall, these findings highlight that CB/PLA is slightly better than other carbon thermoplastics to make reproducible printed parts.

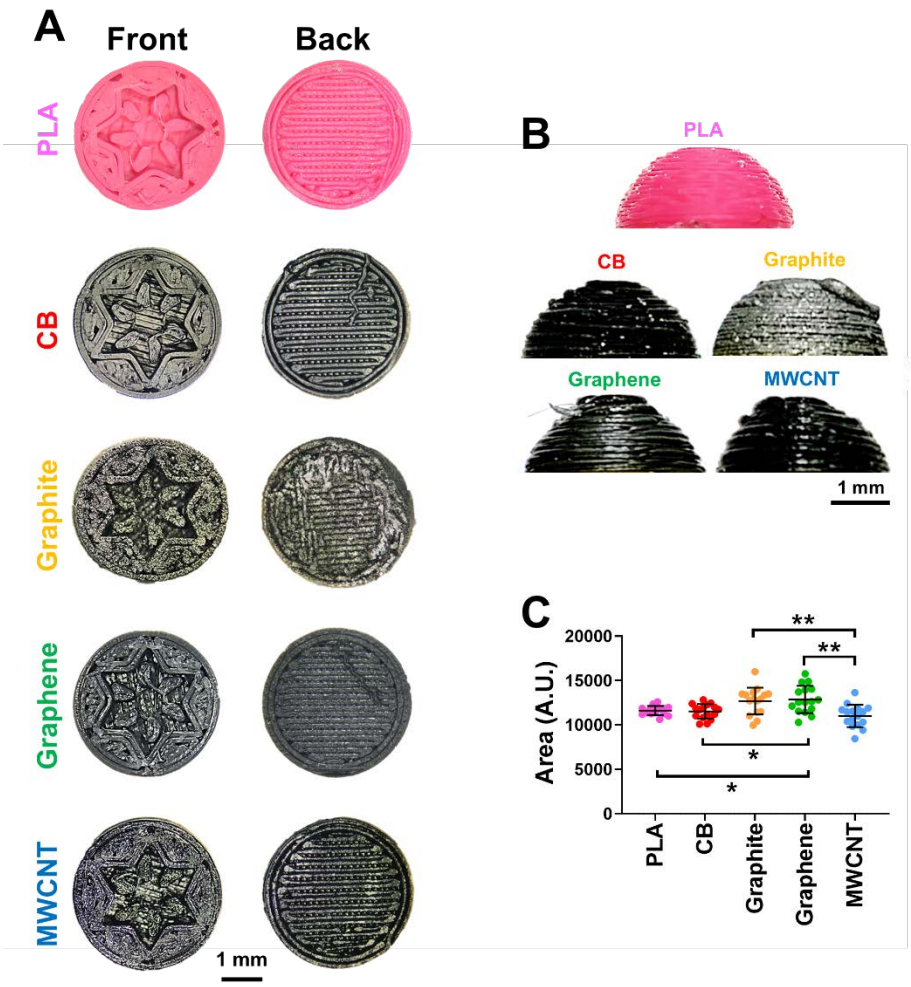

Figure 6. Resolution and batch uniformity of the different carbon allotrope thermoplastic materials when 3D-printed. (A) optical microscopy image of a star design showing the front and back of the printed part on the different carbon thermoplastic materials and PLA, (B) optical microscopy image of the side on view of the 3D printed dome printed using 100 µm print layers for the different materials. (C) Analysis of the surface area of a batch of dome shapes of PLA and all the different carbon allotrope thermoplastic composite materials. Data shown as mean ± S.D, where n=16, *p<0.05, **p<0.01 and ***p<0.001.

CONCLUSIONS

This work showcases the electrochemical comparison of different carbon allotrope thermoplastic composite electrodes. Overall, our studies have eluded that different carbon allotrope thermoplastics composites have varied performance benefits as electrochemical sensing materials. Although, these materials have varying amounts of carbon, there was no direct correlation between the current response and amount of carbon present, highlighting the activity of the carbon allotrope itself influenced the current response. Graphene/PLA was shown to provide the best sensitivity and lowest detection limits for the detection of 5-HT when compared to all other carbon allotrope thermoplastic materials investigated. CB/PLA was least prone to fouling from oxidative by-products from the measurement of 5-HT. CB/PLA was able to print complex shapes with high definition and reproducibility when compared to the other carbon allotrope thermoplastic materials investigated. These findings will provide significant guidance on the appropriate choice of carbon thermoplastic composite material when manufacturing electrochemical sensors.

MATERIALS & METHODS

Chemical and Materials. Potassium chloride, ruthenium (III) chloride hydrate, potassium hexacyanoferrate (III), potassium hexacyanoferrate (II) trihydrate, sodium hydroxide, serotonin creatinine sulfate monohydrate was purchased from Sigma Aldrich. Phosphate-buffered saline (PBS) solution was prepared with 0.01 M disodium hydrogen phosphate, 0.01 M sodium dihydrogen phosphate and 0.9% sodium chloride (Sigma). All the aqueous solutions were prepared

in double distilled water from a Milli-Q. For 3D printing materials we utilised carbon black/PLA filament (marketed as Protopasta and purchased from filaprint, UK), Multi-walled carbon nanotubes (MWCNT)/PLA and carbon fiber/PLA filament (3DX tech, USA) and Graphene/PLA and Graphite/PLA filament (Colfeed, Spain). All filaments were 1.75 mm in diameter.

3D Printing. Electrodes were made using previously published approaches[37-38, 54]. Briefly, a 3D printed cylindrical PLA casing (Raise 3D Pro printer, Irvine, CA), which contained a 2 mm diameter by 1.2 mm depth mold. A coiled copper wire was threaded through the cylinder gap to make the electrical connection. The mold was filled using the different carbon allotrope thermoplastic filaments using a 3D printing pen (SUNLU 300 with a 0.75 mm nozzle) at 180 ºC and 20 mm/s, compressed into the mold and then polished using an abrasive sandpaper 1200 grit and using alumina suspension of 0.30 μm to a smooth surface.

Printed star and dome shapes were made using FlashForge Creator Max Dual Extruder 3D Printer (FlashForge, CA, USA). The print layer thickness was 0.2 mm for the star and 0.1 mm for the dome, printing speed was 3600 mm/s and infill were 100 %. For all materials, the printing conditions are set to those indicated by the material manufacturer.

Apparatus. The optical microscopy was conducted using a stereomicroscope attached to a camera. For the dome, a side-on image was taken, and the outline of the dome was carefully measured using Image J to measure the area.

The percentage mass of carbon present within the thermoplastic filaments was obtained by dissolving the PLA in tetrahydrofuran (THF) to obtain the carbon mass. The resultant suspension was filtered, and sample was weighed dried. To analyze the particle sizes, present in these samples, the dried samples were washed a few times in deionized water, followed by sonication in 10 mL

of the same to ensure adequate dispersion. The wet mixture was then run in a Malvern Instruments Mastersizer (Malvern, UK) with a particle refractive index of 1.416, absorption index of 1.0 and dispersant refractive index of 1.33.

Electrochemical measurements were carried out using CHI760 potentiostat (CH instruments, Texas) monitored using CHI software. All electrochemical measurements were carried out in the conventional three electrode configuration consisting of Ag|AgCl (3 M KCl) reference electrode, Pt wire counter electrode and the varying carbon allotrope thermoplastic electrodes as working electrode. Cyclic voltammetry measurements were carried out using redox probes 1 mM ruthenium (III) hexaamine in 1 M KCl and 1 mM ferricyanide in 1 M KCl at a scan rate of 100 mV s^{-1}. Prior to each measurement, electrochemical precondition of the electrodes was carried out by holding the potential at + 1.4 V for 200s and then at −1.0 V for 200s in 0.5 M NaOH. EIS measurements were carried out using 5 mM ferricyanide and 5 mM ferrocyanide mixture solution 1 M KCl, where the Rct was obtained following fitting the experimental data with a modified Randles-Sevcik equivalent circuit.

Field emission scanning electron microscopy (FE-SEM) images were obtained using a Zeiss SIGMA field emission gun SEM equipped with an Everhart-Thornley detector operating in secondary electron detection mode, using 5 kV accelerating voltage, a 20 µm aperture, and 8.1 mm working distance.

ASSOCIATED CONTENT

Supporting Information. The following files are available free of charge. SEM images of carbon residues obtained following dissolving PLA from the filament using THF, EDS analysis of the carbon allotrope filaments and equivalent circuits utilised to fit the Nyquist and Bode experimental data plots to obtain Rct (PDF)

AUTHOR INFORMATION

Corresponding Author

*Email: b.a.patel@brighton.ac.uk

ORCID

Khalil K. Hussain: 0000-0003-0861-3314

Ricoveer Singh Shergill: 0000-0001-5387-1799

Hairul Hisham Hamzah: 0000-0002-8296-1360

Mark S Yeoman: 0000-0003-2113-8650

Bhavik Anil Patel: 0000-0002-8773-3850

Author Contributions

Khalil Hussain: Methodology, Investigation, Validation, Formal analysis, Writing – original draft. Ricoveer Singh Shergill: Methodology, Investigation, Formal analysis; Hisham Hamzah: Methodology, Investigation, Validation, Formal analysis, Writing – original draft; Mark Yeoman; Writing – review & editing, Supervision, Project administration; Bhavik Anil

Patel: Conceptualization, Methodology, Resources, Formal analysis, Writing – review & editing, Supervision, Project administration.

Funding Sources

The authors would like to thank EPSRC (EP/V028391/1) for funding that supported this study.

Notes

The authors declare no competing financial interest.

ACKNOWLEDGMENT

ABBREVIATIONS

PLA, polylactic acid; CB, carbon black; MWCNT, multiwall carbon nanotubes; CF, carbon fiber

REFERENCES

1. Jian, Z.; Luo, W.; Ji, X., Carbon electrodes for K-ion batteries. *Journal of the American chemical society* **2015,** *137* (36), 11566-11569.
2. Dicks, A. L., The role of carbon in fuel cells. *Journal of Power Sources* **2006,** *156* (2), 128-141.
3. Ratajczak, P.; Suss, M. E.; Kaasik, F.; Béguin, F., Carbon electrodes for capacitive technologies. *Energy Storage Materials* **2019,** *16*, 126-145.

4. Le, T. X. H.; Bechelany, M.; Cretin, M., Carbon felt based-electrodes for energy and environmental applications: A review. *Carbon* **2017,** *122*, 564-591.
5. Joshi, P.; Mishra, R.; Narayan, R. J., Biosensing applications of carbon-based materials. *Current Opinion in Biomedical Engineering* **2021,** *18*, 100274.
6. Wang, J., Carbon-nanotube based electrochemical biosensors: A review. *Electroanalysis: An International Journal Devoted to Fundamental and Practical Aspects of Electroanalysis* **2005,** *17* (1), 7-14.
7. Łukaszewicz, J. P., Carbon materials for chemical sensors: a review. *Sensor Letters* **2006,** *4* (2), 53-98.
8. McCreery, R. L., Advanced carbon electrode materials for molecular electrochemistry. *Chemical reviews* **2008,** *108* (7), 2646-2687.
9. McCreery, R. L.; Cline, K. K., Carbon Electrodes. In *Laboratory techniques in Electroanalytical Chemistry*, Kissinger, P. T.; Heineiman, W. R., Eds. Marcel Dekker: New York, 1996; pp 293 - 332.
10. Pumera, M.; Merkoçi, A.; Alegret, S., Carbon nanotube-epoxy composites for electrochemical sensing. *Sensors and Actuators B: Chemical* **2006,** *113* (2), 617-622.
11. Ramirez-Garcia, S.; Alegret, S.; Cespedes, F.; Forster, R. J., Carbon composite electrodes: surface and electrochemical properties. *Analyst* **2002,** *127* (11), 1512-1519.
12. Tallman, D. E.; Petersen, S. L., Composite electrodes for electroanalysis: Principles and applications. *Electroanalysis* **1990,** *2* (7), 499-510.
13. Wang, J.; Musameh, M., Carbon Nanotube/Teflon Composite Electrochemical Sensors and Biosensors. *Analytical Chemistry* **2003,** *75* (9), 2075-2079.
14. Wang, J.; Naser, N., Modified carbon-wax composite electrodes. *Analytica chimica acta* **1995,** *316* (2), 253-259.
15. Fagan-Murphy, A.; Patel, B. A., Compressed multiwall carbon nanotube composite electrodes provide enhanced electroanalytical performance for determination of serotonin. *Electrochimica Acta* **2014,** *138* (0), 392-399.
16. Zhao, H.; Oâ€™Hare, D., Characterisation and Modeling of Conducting Composite Electrodes. *The Journal of Physical Chemistry C* **2008,** *112* (25), 9351-9357.
17. Henriques, H. P.; Fogg, A. G., Preparation of graphite-loaded epoxy-based voltammetric electrodes using a multi-layer coating and hardening technique. *Analyst* **1984,** *109* (9), 1195-1199.
18. Klatt, L. N.; Connell, D. R.; Adams, R. E.; Honigberg, I. L.; Price, J. C., Voltammetric characterization of a graphite-teflon electrode. *Analytical Chemistry* **1975,** *47* (14), 2470-2472.
19. Mascini, M.; Liberti, A., An analytical study of a new type of halide-sensitive electrode prepared from silver halides and thermoplastic polymers. *Analytica Chimica Acta* **1969,** *47* (2), 339-345.
20. Klunder, K. J.; Nilsson, Z.; Sambur, J. B.; Henry, C. S., Patternable Solvent-Processed Thermoplastic Graphite Electrodes. *Journal of the American Chemical Society* **2017,** *139* (36), 12623-12631.
21. Hamzah, H. H.; Shafiee, S. A.; Abdalla, A.; Patel, B. A., 3D printable conductive materials for the fabrication of electrochemical sensors: A mini review. *Electrochemistry Communications* **2018,** *96*, 27-31.
22. Omar, M. H.; Razak, K. A.; Ab Wahab, M. N.; Hamzah, H. H., Recent progress of conductive 3D-printed electrodes based upon polymers/carbon nanomaterials using a fused deposition modelling (FDM) method as emerging electrochemical sensing devices. *RSC advances* **2021,** *11* (27), 16557-16571.

23. Regel, A.; Lunte, S., Integration of a Graphite/PMMA CompositeElectrode into a Poly (methyl methacrylate)(PMMA) Substrate for Electrochemical Detection in Microchips. *Electrophoresis* **2013,** *34* (14), 2101.
24. Yang, C.; Cao, Q.; Puthongkham, P.; Lee, S. T.; Ganesana, M.; Lavrik, N. V.; Venton, B. J., 3D-Printed Carbon Electrodes for Neurotransmitter Detection. *Angewandte Chemie International Edition* **2018,** *57* (43), 14255-14259.
25. Rabboh, F. M.; O'Neil, G. D., Voltammetric pH Measurements in Unadulterated Foodstuffs, Urine, and Serum with 3D-Printed Graphene/Poly(Lactic Acid) Electrodes. *Analytical Chemistry* **2020,** *92* (22), 14999-15006.
26. Abdalla, A.; Patel, B. A., 3D Printed Electrochemical Sensors. *Annual Review of Analytical Chemistry* **2021,** *14* (1), 47-63.
27. Katseli, V.; Economou, A.; Kokkinos, C., Single-step fabrication of an integrated 3D-printed device for electrochemical sensing applications. *Electrochemistry Communications* **2019,** *103*, 100-103.
28. Manzanares Palenzuela, C. L.; Pumera, M., (Bio)Analytical chemistry enabled by 3D printing: Sensors and biosensors. *TrAC Trends in Analytical Chemistry* **2018,** *103*, 110-118.
29. O'Neil, G. D.; Ahmed, S.; Halloran, K.; Janusz, J. N.; Rodríguez, A.; Terrero Rodríguez, I. M., Single-step fabrication of electrochemical flow cells utilizing multi-material 3D printing. *Electrochemistry Communications* **2019,** *99*, 56-60.
30. Stefano, J. S.; Kalinke, C.; da Rocha, R. G.; Rocha, D. P.; da Silva, V. A. O. P.; Bonacin, J. A.; Angnes, L.; Richter, E. M.; Janegitz, B. C.; Muñoz, R. A. A., Electrochemical (Bio)Sensors Enabled by Fused Deposition Modeling-Based 3D Printing: A Guide to Selecting Designs, Printing Parameters, and Post-Treatment Protocols. *Analytical Chemistry* **2022,** *94* (17), 6417-6429.
31. Cardoso, R. M.; Mendonça, D. M. H.; Silva, W. P.; Silva, M. N. T.; Nossol, E.; da Silva, R. A. B.; Richter, E. M.; Muñoz, R. A. A., 3D printing for electroanalysis: From multiuse electrochemical cells to sensors. *Analytica Chimica Acta* **2018,** *1033*, 49-57.
32. Liyarita, B. R.; Ambrosi, A.; Pumera, M., 3D-printed Electrodes for Sensing of Biologically Active Molecules. *Electroanalysis* **2018,** *30* (7), 1319-1326.
33. Abdalla, A.; Patel, B. A., 3D-printed electrochemical sensors: A new horizon for measurement of biomolecules. *Current Opinion in Electrochemistry* **2020,** *20*, 78-81.
34. Verdier, N.; Foran, G.; Lepage, D.; Prébé, A.; Aymé-Perrot, D.; Dollé, M., Challenges in solvent-free methods for manufacturing electrodes and electrolytes for lithium-based batteries. *Polymers* **2021,** *13* (3), 323.
35. Patel, N.; Fagan-Murphy, A.; Covill, D.; Patel, B. A., 3D Printed Molds Encompassing Carbon Composite Electrodes To Conduct Multisite Monitoring in the Entire Colon. *Analytical Chemistry* **2017,** *89* (21), 11690-11696.
36. Trikantzopoulos, E.; Yang, C.; Ganesana, M.; Wang, Y.; Venton, B. J., Novel carbon-fiber microelectrode batch fabrication using a 3D-printed mold and polyimide resin. *Analyst* **2016,** *141* (18), 5256-5260.
37. Cardoso, R. M.; Castro, S. V.; Stefano, J. S.; Muñoz, R. A., Drawing electrochemical sensors using a 3D printing pen. *Journal of the Brazilian Chemical Society* **2020,** *31*, 1764-1770.
38. Cardoso, R. M.; Rocha, D. P.; Rocha, R. G.; Stefano, J. S.; Silva, R. A. B.; Richter, E. M.; Muñoz, R. A. A., 3D-printing pen versus desktop 3D-printers: Fabrication of carbon black/polylactic acid electrodes for single-drop detection of 2,4,6-trinitrotoluene. *Analytica Chimica Acta* **2020,** *1132*, 10-19.

39. Zaporotskova, I. V.; Boroznina, N. P.; Parkhomenko, Y. N.; Kozhitov, L. V., Carbon nanotubes: Sensor properties. A review. *Modern Electronic Materials* **2016,** *2* (4), 95-105.
40. Yang, C.; Denno, M. E.; Pyakurel, P.; Venton, B. J., Recent trends in carbon nanomaterial-based electrochemical sensors for biomolecules: A review. *Analytica Chimica Acta* **2015,** *887*, 17-37.
41. Zhou, M.; Zhai, Y.; Dong, S., Electrochemical Sensing and Biosensing Platform Based on Chemically Reduced Graphene Oxide. *Analytical Chemistry* **2009,** *81* (14), 5603-5613.
42. Dumitrescu, I.; Unwin, P. R.; Macpherson, J. V., Electrochemistry at carbon nanotubes: perspective and issues. *Chem. Comm.* **2009,** *45*, 6886 - 6901.
43. Guell, A. G.; Meadows, K. E.; Unwin, P. R.; Macpherson, J. V., Trace voltammetric detection of serotonin at carbon electrodes: comparison of glassy carbon, boron doped diamond and carbon nanotube network electrodes. *Physical Chemistry Chemical Physics* **2010,** *12* (34), 10108-10114.
44. Browne, M. P.; Urbanova, V.; Plutnar, J.; Novotný, F.; Pumera, M., Inherent impurities in 3D-printed electrodes are responsible for catalysis towards water splitting. *Journal of Materials Chemistry A* **2020,** *8* (3), 1120-1126.
45. Browne, M. P.; Pumera, M., Impurities in Graphene/PLA 3D-Printing Filaments Dramatically Influence the Electrochemical Properties of the Devices. *Chem. Commun.* **2019,** *55* (58), 8374.
46. Whittingham, M. J.; Crapnell, R. D.; Rothwell, E. J.; Hurst, N. J.; Banks, C. E., Additive Manufacturing for Electrochemical Labs: An Overview and Tutorial Note on the Production of Cells, Electrodes and Accessories. *Talanta Open* **2021,** *4*, 100051.
47. Abdalla, A.; Perez, F.; Cañadas, A. T.; Ray, S.; Patel, B. A., How normalisation factors influence the interpretations of 3D-printed sensors for electroanalysis. *Journal of Electroanalytical Chemistry* **2021,** *881*, 114937.
48. Pereira, J. F. S.; Rocha, R. G.; Castro, S. V. F.; João, A. F.; Borges, P. H. S.; Rocha, D. P.; de Siervo, A.; Richter, E. M.; Nossol, E.; Gelamo, R. V.; Muñoz, R. A. A., Reactive oxygen plasma treatment of 3D-printed carbon electrodes towards high-performance electrochemical sensors. *Sensors and Actuators B: Chemical* **2021,** *347*, 130651.
49. Rocha, D. P.; Ataide, V. N.; de Siervo, A.; Gonçalves, J. M.; Muñoz, R. A. A.; Paixão, T. R. L. C.; Angnes, L., Reagentless and Sub-Minute Laser-Scribing Treatment to Produce Enhanced Disposable Electrochemical Sensors via Additive Manufacture. *Chem. Eng. J.* **2021,** *425* (June), 130594.
50. Veloso, W. B.; Ataide, V. N.; Rocha, D. P.; Nogueira, H. P.; de Siervo, A.; Angnes, L.; Muñoz, R. A.; Paixão, T. R., 3D-printed sensor decorated with nanomaterials by CO2 laser ablation and electrochemical treatment for non-enzymatic tyrosine detection. *Microchim Acta* **2023,** *190* (2), 63.
51. Stefano, J. S.; Silva, L. R. G. e.; Janegitz, B. C., New carbon black-based conductive filaments for the additive manufacture of improved electrochemical sensors by fused deposition modeling. *Microchim Acta* **2022,** *189* (11), 414.
52. Sigley, E.; Kalinke, C.; Crapnell, R. D.; Whittingham, M. J.; Williams, R. J.; Keefe, E. M.; Janegitz, B. C.; Bonacin, J. A.; Banks, C. E., Circular economy electrochemistry: creating additive manufacturing feedstocks for caffeine detection from post-industrial coffee pod waste. *ACS Sustainable Chemistry & Engineering* **2023,** *11* (7), 2978-2988.
53. Rocha, D. P.; Squissato, A. L.; da Silva, S. M.; Richter, E. M.; Munoz, R. A. A., Improved electrochemical detection of metals in biological samples using 3D-printed electrode:

Chemical/electrochemical treatment exposes carbon-black conductive sites. *Electrochimica Acta* **2020,** *335*, 135688.
54. Singh Shergill, R.; Perez, F.; Abdalla, A.; Anil Patel, B., Comparing electrochemical pre-treated 3D printed native and mechanically polished electrode surfaces for analytical sensing. *Journal of Electroanalytical Chemistry* **2022,** *905*, 115994.
55. Hamzah, H. H.; Keattch, O.; Yeoman, M. S.; Covill, D.; Patel, B. A., Three-Dimensional-Printed Electrochemical Sensor for Simultaneous Dual Monitoring of Serotonin Overflow and Circular Muscle Contraction. *Analytical Chemistry* **2019,** *91* (18), 12014-12020.
56. Spohn, S. N.; Mawe, G. M., Non-conventional features of peripheral serotonin signalling — the gut and beyond. *Nature Reviews Gastroenterology &Amp; Hepatology* **2017,** *14*, 412.
57. Patel, B. A., Electroanalytical approaches to study signaling mechanisms in the gastrointestinal tract. *Neurogastroenterology & Motility* **2011,** *23* (7), 595-605.
58. Dankoski, E. C.; Wightman, R. M., Monitoring serotonin signaling on a subsecond time scale. *Frontiers in integrative neuroscience* **2013,** *7*, 44.
59. Roberts, J. G.; Sombers, L. A., Fast scan cyclic voltammetry: Chemical sensing in the brain and beyond. *Analytical chemistry* **2018,** *90* (1), 490.
60. Ou, Y.; Buchanan, A. M.; Witt, C. E.; Hashemi, P., Frontiers in electrochemical sensors for neurotransmitter detection: towards measuring neurotransmitters as chemical diagnostics for brain disorders. *Analytical Methods* **2019,** *11* (21), 2738-2755.
61. Brooks, E. L.; Hussain, K. K.; Kotecha, K.; Abdalla, A.; Patel, B. A., Three-Dimensional-Printed Electrochemical Multiwell Plates for Monitoring Food Intolerance from Intestinal Organoids. *ACS Sensors* **2023**.
62. Patel, B. A.; Bian, X.; Quaiserova-Mocko, V.; Galligan, J. J.; Swain, G. M., *In vitro* continuous amperometric monitoring of 5-hydroxytryptamine release from enterochromaffin cells of the guinea pig ileum. *The Analyst* **2007,** *132* (1), 41-47.
63. Swamy, B. E. K.; Venton, B. J., Carbon nanotube-modified microelectrodes for simultaneous detection of dopamine and serotonin in vivo. *The Analyst* **2007,** *132* (9), 876-884.
64. Yang, C.; Trikantzopoulos, E.; Jacobs, C. B.; Venton, B. J., Evaluation of carbon nanotube fiber microelectrodes for neurotransmitter detection: Correlation of electrochemical performance and surface properties. *Analytica chimica acta* **2017,** *965*, 1-8.
65. Cernat, A.; Ştefan, G.; Tertis, M.; Cristea, C.; Simon, I., An overview of the detection of serotonin and dopamine with graphene-based sensors. *Bioelectrochemistry* **2020,** *136*, 107620.
66. Dryhurst, G., Applications of electrochemistry in studies of the oxidation chemistry of central nervous system indoles. *Chemistry Reviews* **1990,** *90*, 795 - 811.
67. Wrona, M. Z.; Dryhurst, G., Oxidation chemistry of 5-hydroxytryptamine. 1. Mechanism and products formed at micromolar concentrations. *The Journal of Organic Chemistry* **1987,** *52* (13), 2817 -2825.
68. Wrona, M. Z.; Dryhurst, G., Oxidation chemistry of 5-hydroxytryptamine : Part II. Mechanisms and products formed at millimolar concentrations in acidic aqueous solution. *Journal of Electroanalytical Chemistry* **1990,** *278* (1-2), 249-267.
69. Perez, F.; Kotecha, N.; Lavoie, B.; Mawe, G. M.; Patel, B. A., Monitoring Gut Epithelium Serotonin and Melatonin Overflow Provides Spatial Mapping of Inflammation. *ChemBioChem n/a* (n/a), e202200334.
70. Fagan-Murphy, A.; Watt, F.; Morgan, K. A.; Patel, B. A., Influence of different biological environments on the stability of serotonin detection on carbon-based electrodes. *Journal of Electroanalytical Chemistry* **2012,** *684* (0), 1-5.

71. Ye, W.; Wu, W.; Hu, X.; Lin, G.; Guo, J.; Qu, H.; Zhao, J., 3D printing of carbon nanotubes reinforced thermoplastic polyimide composites with controllable mechanical and electrical performance. *Composites Science and Technology* **2019,** *182*, 107671.
72. Devicharan, R.; Garg, R., Optimization of the print quality by controlling the process parameters on 3D printing machine. In *3D Printing and Additive Manufacturing Technologies*, Springer: 2019; pp 187-194.
73. Abdalla, A.; Hamzah, H.; Keattch, O.; Covill, D.; Patel, B., Augmentation of conductive pathways in carbon black/PLA 3D-printed electrodes achieved through varying printing parameters. *Electrochimica Acta* **2020,** *354*, 136618.